

Development of tracking and focusing micro actuators for dual-stage optical pick-up head

Mingching Wu, Sheng-Yi Hsiao, Chih-Yu Peng and Weileun Fang

Department of Power Mechanical Engineering, National Tsing Hua University, Hsinchu, Taiwan

E-mail: fang@pme.nthu.edu.tw

Received 14 September 2005, accepted for publication 9 December 2005

Published 31 May 2006

Online at stacks.iop.org/JOptA/8/S323

Abstract

This work presents a miniaturized tracking and focusing optical pickup head implemented using MEMS technology. The device was fabricated by poly-Si trench-refilled technology and used a UV-cured polymer droplet or micro ball lens as the objective lens. A bidirectional vertical comb-drive actuator and V-beam thermal actuator drove the objective lens for the out-of-plane (focusing) and in-plane (tracking) motion, respectively. In applications, various tracking and focusing devices have been successfully fabricated and characterized. The upward and downward displacement of the focusing optical pickup head is 2.9 and 1.7 μm , respectively; the in-plane displacement of the tracking optical pickup head is $\pm 46.7 \mu\text{m}$. The resonant frequencies of the focusing and tracking systems are 2.3 and 8.5 kHz respectively. In addition, the UV-cured polymer lens and solid micro ball lens were both successfully integrated with a MEMS device to create an objective lens.

Keywords: MEMS, optical pickup head, vertical comb-drive actuator

(Some figures in this article are in colour only in the electronic version)

1. Introduction

Due to the demands of information technology and personal commercial products, compact and high density data storage systems have been the key technology of the state-of-the-art. Recently, several approaches to high density data storage have been widely investigated based on MEMS technologies, such as the magnetic hard-disk drive [1–3], magnetic-optical recording [4], and modified AFM (atomic force microscope) [5, 6]. An optical data storage system is another key solution for increasing data density for the next generation. A high numerical aperture (NA) optical system substantially increases the storage density in terms of smaller optical spot. However, such high storage density requires a very high bandwidth servo-tracking system to precisely position the optical pickup head in a narrow track spacing ($\sim 100 \text{ nm}$). One promising solution is to develop micro actuators for nanoscale positioning.

The development of an optical pickup head using MEMS technology has been demonstrated extensively. Various optical

elements have been integrated on a micro optical bench by means of micromachining process [7, 8]. Piezoelectric actuators [9] and bimorph thermal actuators [10] have been exploited for data tracking. Moreover, electrostatic vertical comb-drive actuators for optical focusing have been demonstrated in [11, 12]. The concept of integrating UV-cured polymer lenses with MEMS actuators has also been demonstrated in [13]. In this case, the in-plane and out-of-plane positioning actuators are integrated by means of bonding technique. However, the travelling distance of the micro-actuator remains one of the primary design considerations. The concept of a dual-stage slider was first presented in [14] for hard-disk data storage systems. In order to improve the travelling distance and response, a more complete dual-stage system was further demonstrated in [3] for a hard-disk drive. The simple and efficient method of a dual-stage servo controller is also demonstrated in [15].

In general, a dual-stage optical storage system consists of a conventional voice coil motor (VCM) and MEMS actuators. The conventional VCM actuator acts as a coarse, low-speed,

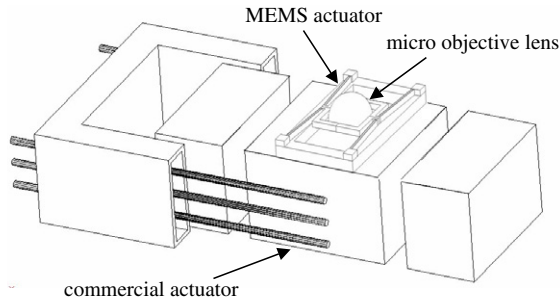


Figure 1. Schematic diagram of proposed dual-stage optical data storage system.

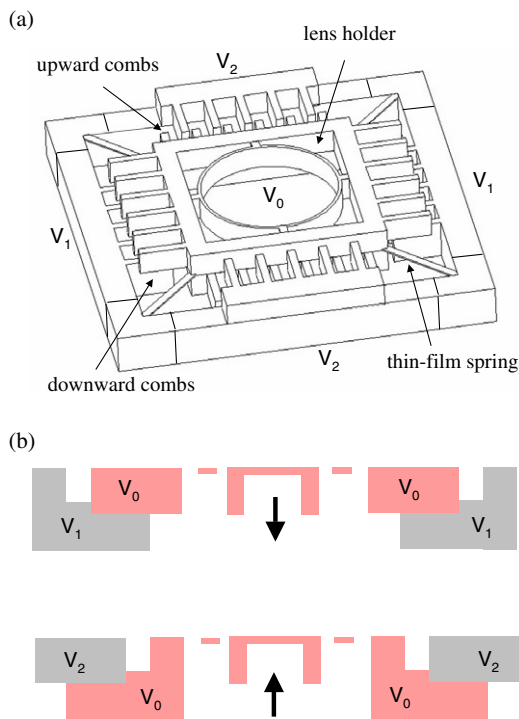


Figure 2. Proposed focusing optical pickup head: (a) schematic diagram of the device, and (b) the principle of bidirectional actuation.

but large-stroke positioner, whereas the MEMS actuator acts as a fine, high-speed, but small-stroke positioner. The integration of the VCM and MEMS actuators will satisfy the requirements of travelling distance, precision positioning, and fast response for data speed and density. The goal of this study is to develop MEMS actuators of a dual-stage optical storage system for small displacement ($\sim 10 \mu\text{m}$) precision tracking and focusing. In short, a novel bidirectional vertical comb MEMS actuator acts as a focusing positioner, and the V-beam thermal MEMS actuator serves as a tracking positioner.

2. Concepts and design

This concept of the presented dual-stage optical storage system is shown in figure 1. In this dual-stage system, the MEMS device is designed to attach to a conventional actuator. The MEMS device consists of micro actuators, a lens holder,

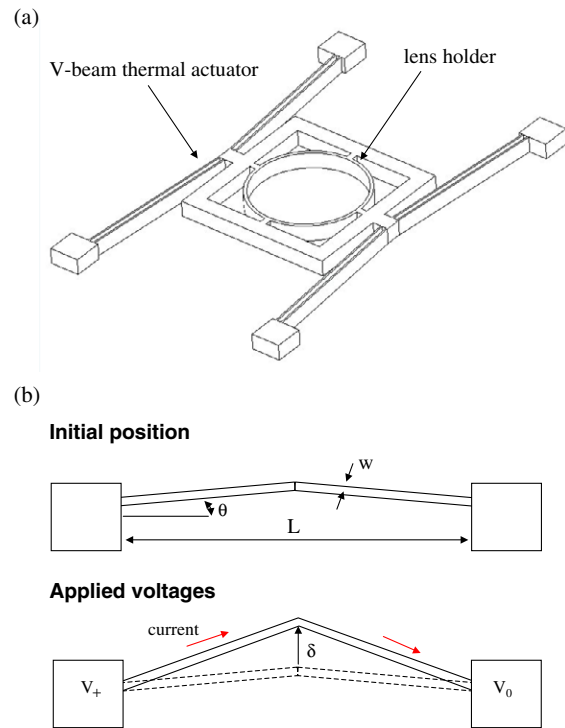


Figure 3. Proposed tracking optical pickup head: (a) schematic diagram of the device, and (b) the parameter definitions of the V-beam thermal actuator.

and a UV-cured polymer lens (or a micro ball lens). The incident light beam is focused by the micro objective lens and modulated by the MEMS and conventional actuators. Figure 2(a) shows a schematic illustration of the present MEMS focusing device. A movable lens holder is connected to a stationary rigid frame by four thin film springs. The lens holder is designed to place the micro lens. The out-of-plane position of the lens holder, regardless of upward or downward directions, is tuned by two pairs of vertical comb actuators (named upward and downward combs in figure 2(a)). As indicated in figure 2(a), the moving electrodes are located below the stationary electrodes for the upward combs, whereas the moving electrodes are located above the stationary electrodes for the downward combs. The stationary electrodes of the upward and downward combs are electrically isolated and can be individually actuated, and the moving electrodes are grounded through thin film springs. Figure 2(b) shows that the upward motion is actuated by V_0 and V_1 , while the downward motion is actuated by V_0 and V_2 . Moreover, the thickness and location of the vertical comb electrodes are tunable by the process to improve the travelling distance and driving voltage [16]. In this design, the thicknesses of the movable combs and stationary combs are both $20 \mu\text{m}$, so that the expected travelling distance is $20 \mu\text{m}$.

The travelling distance could be limited by the side-sticking effect due to the misalignment of the comb electrodes [17]. In this work, the self-aligned vertical combs technique is adopted to prevent misalignment of the electrodes [18]. The in-plane to out-of-plane stiffness ratio of the thin film spring in figure 2(a) will also influence the occurrence of side-sticking. The in-plane to out-of-plane

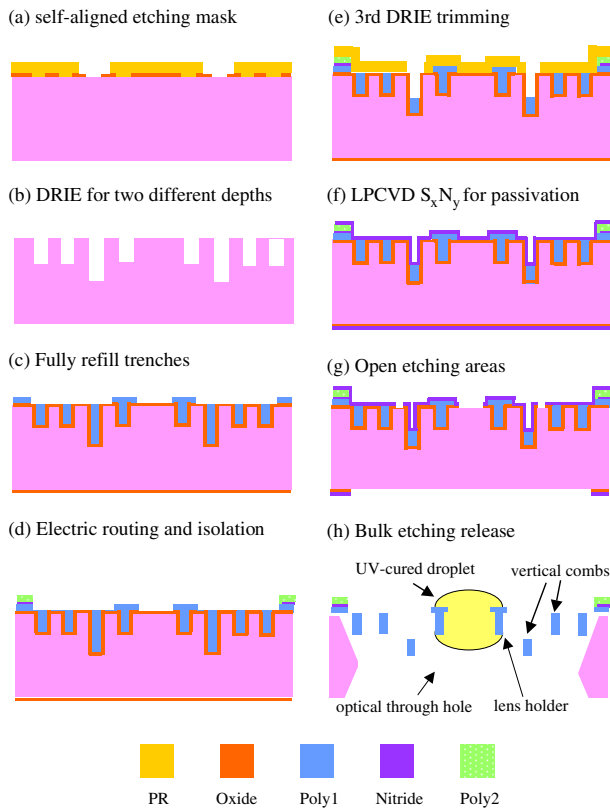


Figure 4. Fabrication process steps.

stiffness ratio K_{ratio} of a thin film spring with thickness t and width w is $(w/t)^2$. In this design, the beam width w is $20 \mu\text{m}$ and the thickness t is $2 \mu\text{m}$, so K_{ratio} is near 1000. Therefore, the side-sticking effect can be suppressed by thin film springs.

As figure 3(a) shows, the proposed in-plane motion tracking device consists of V-beam thermal actuators [19] and a lens holder. After the thermal expansion of the V-beam by joule heating, the actuator will push the lens holder in the in-plane direction. The V-beam actuators located at both sides of lens holder are employed to move the light beam in the opposite direction. The travelling distance of the actuator is determined by the beam length L and angle θ , as figure 3(b) shows. When voltage is applied across V-beam structures, the electrical current leads to joule heating in the V-beam structures. Therefore, the thermal expansion of V-beam structures would generate an in-plane displacement, as indicated by δ in figure 3(b). In the present design, L is $2000 \mu\text{m}$ and θ is 1° . According to the finite element method (FEM) simulation results, the maximum travelling distance (δ) is near $40 \mu\text{m}$. In addition, the inclined V-beams also serve as the suspension mechanism of the device. In this design, the V-beam width w is $2 \mu\text{m}$ and the thickness t is $20 \mu\text{m}$, so the in-plane to out-of-plane stiffness ratio K_{ratio} is near 0.001. This indicates that the V-beam is appropriate to act as an in-plane spring.

3. Fabrication and results

It is a real challenge to fabricate the device in figure 2(a) with various out-of-plane dimensions. The fabrication processes

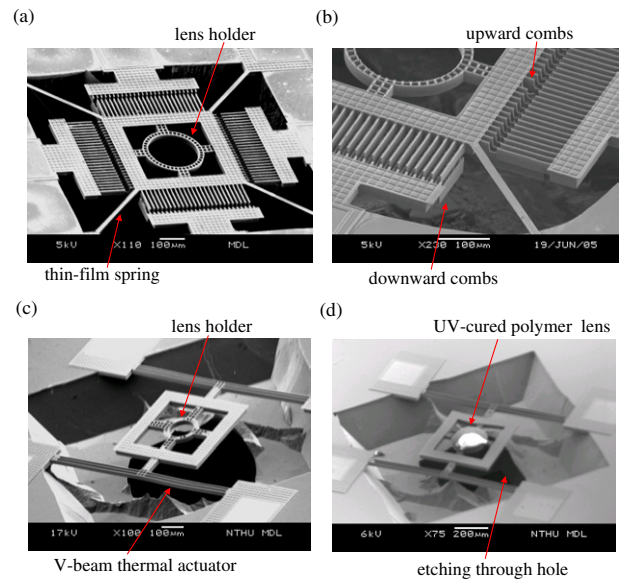


Figure 5. Fabrication results of the proposed optical pickup head: (a) bird's eye view of the focusing optical pickup head, (b) close-up view of bidirectional actuators, (c) the tracking optical pickup head, and (d) UV-cured polymer lens integrated with the releasing device.

employed in this study are illustrated in figure 4. The processes began with the deposition and patterning of thermal oxide, as shown in figure 4(a). A second photolithography was used to define the location of deeper trenches. The patterned thermal oxide and photoresist were used as the self-aligned etching masks for the following DRIE (deep reactive ion etching). The photoresist in figure 4(a) was removed after the first DRIE. The silicon oxide acted as the etching mask for the second DRIE. The silicon substrate had self-aligned trenches with two different depths for the vertical comb electrodes after the second DRIE, as shown in figure 4(b). After that, these trenches were fully refilled by thermal oxide and first LPCVD (low pressure chemical vapour deposition) poly-Si films, as shown in figure 4(c). After the first poly-Si was patterned, the Si_xN_y sacrificial layer and second poly-Si structural layer were deposited and patterned, as shown in figure 4(d). The Si_xN_y and second poly-Si also served as electrical interconnections for the electrically isolated comb electrodes. After being patterned with photoresist, the third DRIE was exploited to etch the first poly-Si, as shown in figure 4(e). The thickness of the trench-refilled poly-Si was trimmed, and the initial engagement of the comb electrodes was defined. Hence micromachined structures located at different out-of-plane positions became available, so as to realize the vertical comb electrodes. In addition, the V-beam thermal actuators and lens holder were also implemented using the shallow refilled trenches. In figures 4(f), (g), we see that low stress nitride was deposited and patterned as the etching mask for bulk silicon etching. Meanwhile, the poly-Si film was fully covered by the thermal oxide and the Si_xN_y films. The substrate was then immersed into tetra-methyl ammonium hydroxide solution for bulk silicon etching. The thermal oxide and the Si_xN_y performed as passivation layers for the poly-Si structure during double-side bulk silicon etching. A hole was available for the incident light to pass through the wafer.

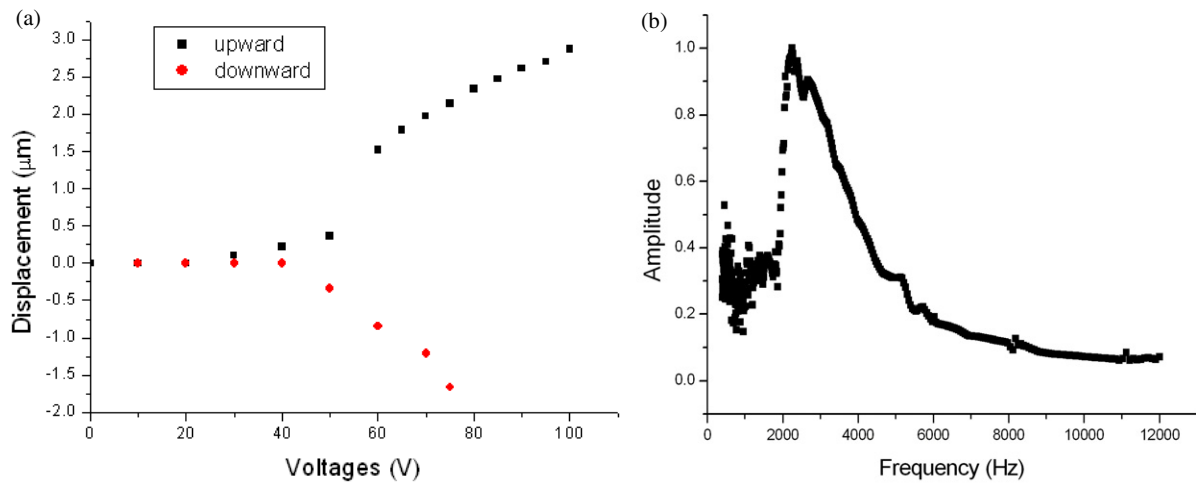


Figure 6. Measured results of focusing optical pickup head: (a) the static load–deflection test for upward and downward actuation, and (b) the frequency response of the device.

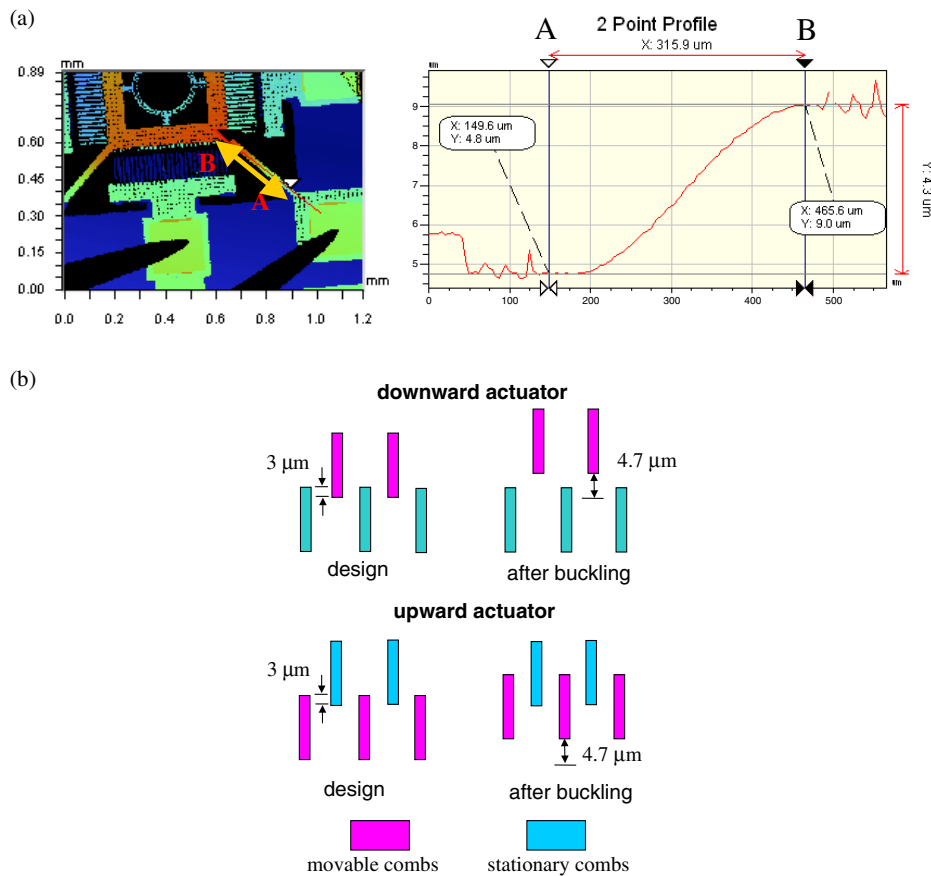


Figure 7. Result of profile measurement by optical interferometer: (a) the poly-Si spring had 4.7 µm displacement after buckling, and (b) schematic diagram of the resulting initial position of the vertical comb drive electrodes.

Finally, the passivation layers were removed and the UV-cured polymer droplet was dropped into the lens holder, as shown in figure 4(h).

Figure 5 shows various typical fabrication results. Figure 5(a) shows the focusing MEMS device. The close-up photograph in figure 5(b) shows the upward and downward combs, stiff lens holder, and flexible film–film poly-Si springs.

The initial engagement available by the third DRIE trimming is 3 µm to provide a larger electrostatic driving force. Figure 5(c) shows the tracking MEMS device including the V-beam actuators and the lens holder. The UV-cured polymer lens was successfully placed in a lens holder with a diameter of 200 µm, as shown in figure 5(d).

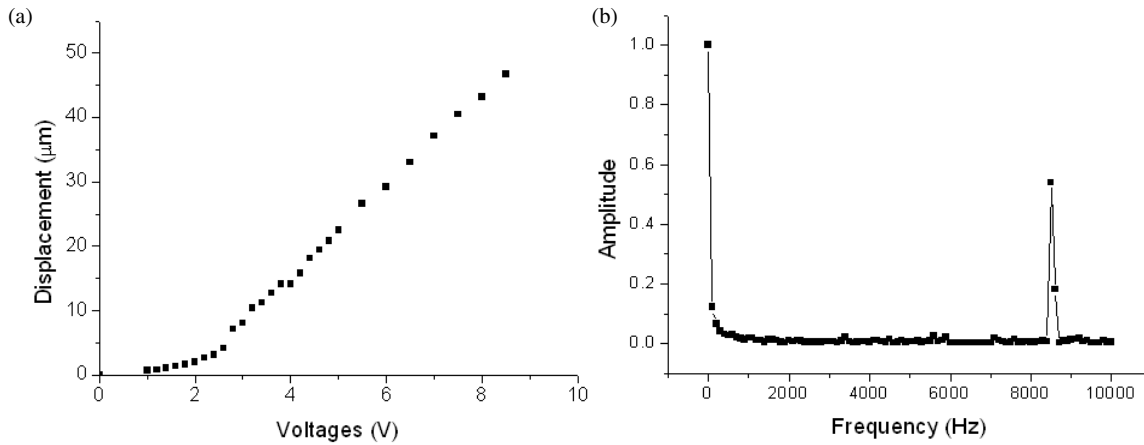


Figure 8. Measured results of tracking optical pickup head: (a) the static load–deflection test for in-plane actuation, and (b) the frequency response of the device.

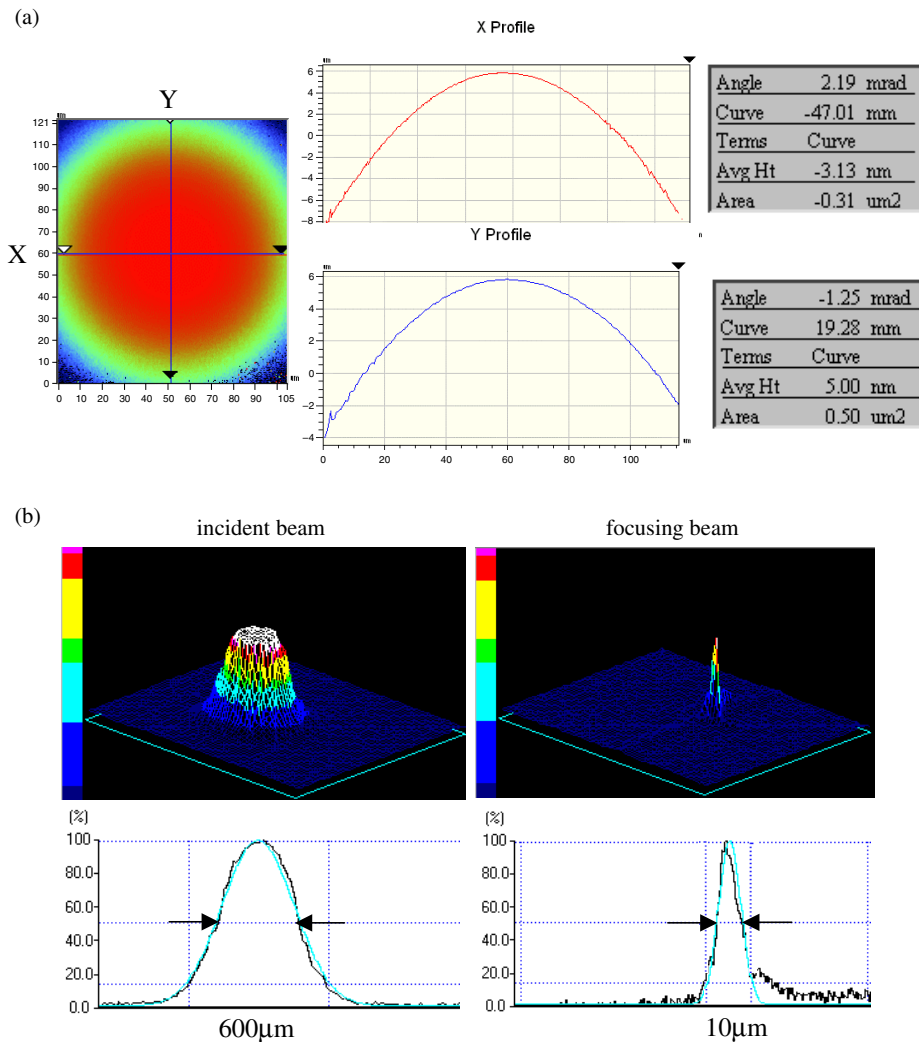


Figure 9. Optical property of UV-cured polymer lens: (a) the surface roughness of the lens measured by an optical interferometer, and (b) the intensity profiles of the incident beam and focusing beam.

4. Testing

To demonstrate the performance of the proposed devices, the static and dynamic characteristics of the fabricated MEMS

devices were measured. The device was driven by DC voltage for static load–deflection tests, and by AC voltage for dynamic resonant tests. The out-of-plane displacement of the focusing

device was measured by an optical interferometer, and the typical measured results are shown in figure 6. The maximum upward displacement of the device was $2.9 \mu\text{m}$ when the driving voltage reached 100 V, and the maximum downward displacement was $1.7 \mu\text{m}$ when the driving voltage was 75 V, as shown in figure 6(a). An optical laser Doppler vibrometer was used to measure the out-of-plane dynamic response of the devices. The frequency response of the focusing device is shown in figure 6(b), and the resonant frequency associated with the first out-of-plane spring bending mode is 2.3 kHz.

The thickness of the electrodes was $20 \mu\text{m}$; hence the ideal travelling distance of focusing device was also $20 \mu\text{m}$. However, the measured maximum displacements in figure 6(a) were much smaller than the predicted ones. The measurement results in figure 7(a) show that the poly-Si springs had an initial buckling of $4.3 \mu\text{m}$ (upward) by residual compression. The initial positions of the lens holder and the moving electrodes were also moved upward. Thus the initial engagement of electrodes as illustrated in figure 7(b) and the associated driving voltages were all changed. In addition, the spring stiffness was also increased by the initial deformation. Some stress engineering [20] or stress releasing structure [21] would be useful to improve the residual stress and prevent this phenomenon.

The in-plane displacement of the tracking device was measured using a commercial in-plane micro motion analyser. Figure 8(a) shows a typical measurement result of a static load–deflection test. The in-plane displacement of the device driven by a single-side V-beam actuator was $46.7 \mu\text{m}$ when the driving voltage was 8.5 V. The frequency response in figure 8(b) shows that the first resonant frequency of a typical tracking device is 8.5 kHz. The frequency response also indicates that the MEMS device has a quick response and a high bandwidth for a servo-tracking system.

The optical properties of the UV-cured polymer lens were also measured. Figure 9(a) indicates the surface profile of the UV-cured polymer lens that was measured by an optical interferometer. The average surface roughness of the x -axis and y -axis was 3.13 and 5 nm, respectively. Moreover, the surface roughness of the polymer lens measured by AFM was also less than 10 nm. Therefore, the polymer lens provided a good surface for optical applications. In addition, the intensity profiles of the focused beam were measured by the beam profiler, as indicated in figure 9(b). A laser beam was incident on the UV-cured polymer lens (diameter $\sim 600 \mu\text{m}$) from the backside of the substrate, and then focused on a beam profiler by the polymer lens. The spot size of the incident beam and focusing beam is ~ 600 and $\sim 10 \mu\text{m}$ (full width at half maximum), respectively. The focused spot size of the available UV-cured polymer lens was far from the optical requirements. In this regard, this study also demonstrated another approach that used the MEMS structure (lens holder) to integrate a commercial high NA objective lens. Figure 10(a) shows the integration of a micro ball lens (size $\sim 250 \mu\text{m}$) and a MEMS focusing actuator. The micro ball lens was picked by vacuum handler and assembled on the lens holder. Thus, the optical properties of the miniaturized MEMS pickup can be significantly improved. Lastly, figure 10(b) demonstrates the system integration of a dual-stage optical pickup head consisting of a MEMS tracking positioner and

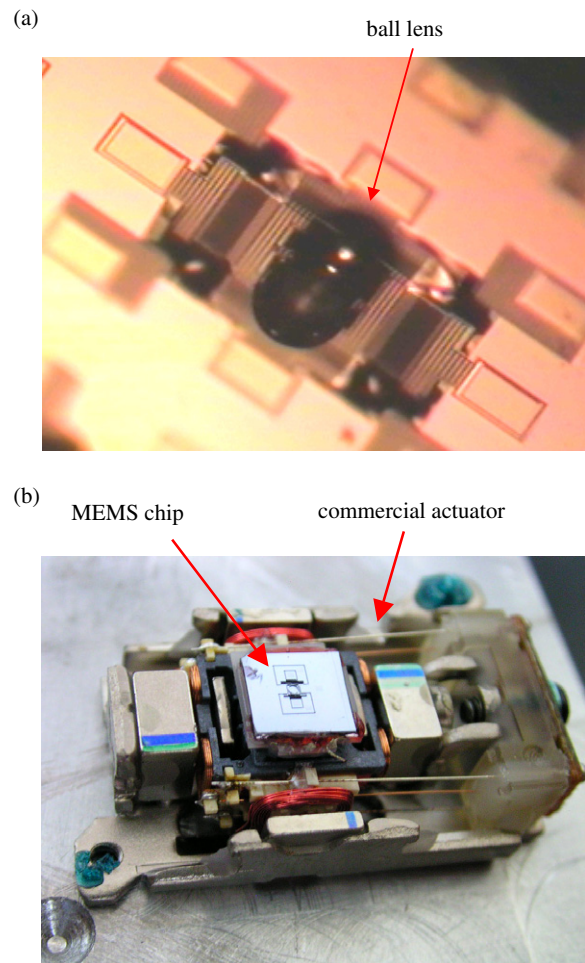


Figure 10. (a) A micro ball lens was integrated with focusing optical pickup head, and (b) the system integration of a dual-stage optical pickup consisting of a MEMS tracking positioner and a conventional actuator.

a conventional VCM actuator. The objective lens of the conventional optical pickup head was replaced by the MEMS positioner and polymer lens. The integration of the VCM and MEMS positioner will satisfy the requirements of travelling distance, precision positioning, and fast response for data speed and density.

5. Conclusions

This study has demonstrated focusing and tracking MEMS devices for an optical pickup head. Novel fabrication processes have been established to realize MEMS devices with various out-of-plane dimensions. The comb electrodes are self-aligned by the present process; moreover, the initial engagement of the vertical comb electrodes is tunable. In addition, other key components such as the lens holder and the V-beam thermal actuator are also available through this process. The thin-film suspension and electrically isolated interconnection are available through poly-Si and dielectric Si_xN_y . The measurement results show that the present MEMS devices have a quick response and a high bandwidth. The surface roughness of the UV-cured polymer lens is less than 10 nm. In additions, the UV-cured polymer lens and solid micro ball lens were both

successfully integrated with a MEMS device. In summary, the dual-stage optical pickup head consisting of a MEMS tracking positioner and a conventional VCM actuator will significantly increase data speed and density for next generation optical data storage system. This study also demonstrates the potential of integrating various optical components (e.g. MEMS actuators and micro-optics) fabricated using different techniques. Thus the design of high performance opto-mechanical systems becomes more flexible.

Acknowledgments

This paper was (partially) supported by the Ministry of Economic Affairs, Taiwan, under contract No. 93-EC-17-A-07-S1-0011, and by National Science Council, Taiwan, under contract NSC 93-2215-E-007-005. The authors would also like to thank the NSC Central Regional MEMS Center (Taiwan), the Nano Facility Center of National Tsing Hua University, and the NSC National Nano Device Laboratory (NDL) for providing the fabrication facilities.

References

- [1] Fan L-S, Ottesen H H, Reiley T C and Wood R W 1995 Magnetic recording-head positioning at very high track densities using a microactuator-based, two-stage servo system *IEEE Trans. Ind. Electron.* **42** 222–33
- [2] Hirano T, Fan L-S, Gao J Q and Lee W Y 1998 MEMS milliactuator for hard-disk-drive tracking servo *J. MEMS* **7** 149–55
- [3] Toshiyoshi H, Mita M and Fujita H 2002 A MEMS piggyback actuator for hard-disk drives *J. MEMS* **11** 648–64
- [4] Hata S, Yamada Y, Ichihara J and Shimokohbe A 2002 A micro lens actuator for optical flying head *IEEE MEMS'02 (Las Vegas, CA, USA)* (Piscataway, NJ: IEEE) pp 507–10
- [5] Vettiger P *et al* 2002 The millipede —nanotechnology entering data storage *IEEE Trans. Nanotechnol.* **1** 39–55
- [6] Despont M, Drechsler U, Yu R, Pogge H B and Vettiger P 2004 Wafer-scale microdevice transfer/interconnect: its application in an AFM-based data-storage system *J. MEMS* **13** 895–901
- [7] Lin L Y, Shen J L, Lee S S and Wu M C 1996 Realization of novel monolithic free-space optical disk pickup heads by surface-micromachining *Opt. Lett.* **21** 155–7
- [8] Tseng F G and Hu H T 2003 A novel micro optical system employing inclined polymer mirrors and Fresnel lens for monolithic integration of optical disk pickup heads *IEEE Transducers'03 (Boston, USA)* (Piscataway, NJ: IEEE) pp 599–602
- [9] Yee Y, Nam H-J, Lee S-H, Bu J U, Jeon Y-S and Cho S-M 2000 PZT actuated micromirror for nano-tracking of laser beam for high-density optical data storage *IEEE MEMS'00 (Miyazaki, Japan)* (Piscataway, NJ: IEEE) pp 435–8
- [10] Yang J P, Deng X C and Chong T C 2005 An electro-thermal bimorph-based microactuator for precise track-positioning of optical disk drives *J. Micromech. Microeng.* **15** 958–65
- [11] Kim S-H, Yee Y, Choi J, Kwon H, Ha M-H, Oh C and Bu J U 2003 Integrated micro optical flying head with lens positioning actuator for small form factor data storage *IEEE Transducers'03 (Boston, USA)* (Piscataway, NJ: IEEE) pp 607–10
- [12] Kim S-H, Yee Y, Choi J, Kwon H, Ha M-H, Oh C and Bu J U 2004 A micro optical flying head for PCMCIA-sized optical data storage *IEEE MEMS'04 (Maastricht, Netherlands)* (Piscataway, NJ: IEEE) pp 85–8
- [13] Kwon S, Milanović V and Lee L P 2002 Large-displacement vertical microlens scanner with low driving voltage *IEEE Photon. Technol. Lett.* **14** 1572–4
- [14] Wickert J A, Lambeth D N and Fang W 1991 Towards a micromachined dual slider and suspension assembly for contact recording *STLE/ASME Tribology Conf. (St. Louis, MO, USA, 1991)* pp 27–39
- [15] Semba T, Hirano T, Hongt J and Fan L-S 1999 Dual-stage servo controller for HDD using MEMS microactuator *IEEE Trans. Magn.* **35** 2271–3
- [16] Tsai J M-L, Chu H-Y, Hsieh J and Fang W 2004 The BELST II process for silicon HARM vertical comb actuator and its applications *J. Micromech. Microeng.* **15** 535–42
- [17] Tsuboi O, Mizuno Y, Koma N, Soneda H, Okuda H, Ueda S, Sawaki I and Yamagishi F 2002 A rotational comb-driven micromirror with a large deflection angle and low drive voltage *IEEE MEMS'02 (Las Vegas, NV, USA)* (Piscataway, NJ: IEEE) pp 532–5
- [18] Wu M, Lai C-F and Fang W 2005 Design and fabrication of MEMS devices using the integration of MUMPs, trench-refilled molding, DRIE and bulk silicon etching processes *J. Micromech. Microeng.* **15** 535–42
- [19] Sinclair M J 2000 A high force low area MEMS thermal actuator *Int. Society Conf. on Thermal Phenomena (Las Vegas, NV, USA)* pp 127–32
- [20] Yang J, Kahn H, He A-Q, Phillips S M and Heuer A H 2000 A new technique for producing large-area as-deposited zero-stress LPCVD polysilicon films: the multipoly process *J. MEMS* **9** 485–94
- [21] Greywall D S, Busch P A, Pardo F, Carr D W, Bogart G and Soh H T 2003 Crystalline silicon tilting mirrors for optical cross-connect switches *J. MEMS* **12** 708–12